

Fault-Tolerant Quantum Dynamical Decoupling

K. Khodjasteh¹ and D.A. Lidar^{2,3}

¹*Physics Department, University of Toronto, 60 St. George St., Toronto, Ontario, Canada M5S 1A7*

²*Chemistry Department, University of Toronto, 80 St. George St., Toronto, Ontario, Canada M5S 3H6 and*

³*Current address: Chemistry and Electrical Engineering Departments,
University of Southern California, Los Angeles, CA 90089*

Dynamical decoupling pulse sequences have been used to extend coherence times in quantum systems ever since the discovery of the spin-echo effect. Here we introduce a method of recursively concatenated dynamical decoupling pulses, designed to overcome both decoherence and operational errors. This is important for coherent control of quantum systems such as quantum computers. For bounded-strength, non-Markovian environments, such as for the spin-bath that arises in electron- and nuclear-spin based solid-state quantum computer proposals, we show that it is strictly advantageous to use concatenated, as opposed to standard periodic dynamical decoupling pulse sequences. Namely, the concatenated scheme is both fault-tolerant and super-polynomially more efficient, at equal cost. We derive a condition on the pulse noise level below which concatenated is guaranteed to reduce decoherence.

PACS numbers: 03.67.-a, 02.70.-c, 03.65.Yz, 89.70.+c

Introduction.— In spite of considerable recent progress, coherent control and quantum information processing (QIP) is still plagued by the problems associated with controllability of quantum systems under realistic conditions. The two main obstacles in any experimental realization of QIP are (i) *faulty controls*, i.e., control parameters which are limited in range and precision, and (ii) *decoherence-errors* due to inevitable system-bath interactions. Nuclear magnetic resonance (NMR) has been a particularly fertile arena for the development of many methods to overcome such problems, starting with the discovery of the spin-echo effect, and followed by methods such as refocusing, and composite pulse sequences [1]. Closely related to the spin-echo effect and refocusing is the method of dynamical decoupling (DD) pulses introduced into QIP in order to overcome decoherence-errors [2, 3]. In standard DD one uses a *periodic* sequence of fast and strong symmetrizing pulses to reduce the undesired parts of the system-bath interaction Hamiltonian H_{SB} , causing decoherence. Since DD requires no encoding overhead, no measurements, and no feedback, it is an economical alternative to the method of quantum error correcting codes (QECC) [e.g., [4, 5, 6], and references therein], in the non-Markovian regime [7].

Here we introduce *concatenated* DD (CDD) pulse sequences, which have a recursive temporal structure. We show both numerically and analytically that CDD pulse sequences have two important advantages over standard, periodic DD (PDD): (i) Significant fault-tolerance to both random and systematic pulse-control errors (see Ref. [8] for a related study), (ii) CDD is significantly more efficient at decoupling than PDD, when compared at equal switching times and pulse numbers. These advantages simplify the requirements of DD (fast-paced strong pulses) in general, and bring it closer to utility in QIP as a feedback-free error correction scheme.

The noisy quantum control problem.— The problem of

faulty controls and decoherence errors in the context of QIP, as well as other quantum control scenarios [9], can be formulated as follows. The total Hamiltonian H for the control-target system (S) coupled to a bath (B) may be decomposed as: $H = H_S \otimes I_B + I_S \otimes H_B + H_{SB}$, where I is the identity operator. The component H_{SB} is responsible for decoherence in S . We focus here on the single qubit case, but the generalization to many qubits, with H_{SB} containing only single qubit couplings, is straightforward. We shall interchangeably use X, Y, Z to denote the corresponding Pauli matrices σ_α , and σ_0 to denote I . The system Hamiltonian is $H_S = H_S^{\text{int}} + H_P$, where H_S^{int} is the intrinsic part (self Hamiltonian), and H_P is an externally applied, time-dependent control Hamiltonian. We denote all the uncontrollable time-independent parts of the total Hamiltonian by H_e , the “else” Hamiltonian: $H_e := H_S^{\text{int}} + H_B + H_{SB}$. We assume that all operators, except I , are traceless (traceful operators can always be absorbed into $H_S \otimes I_B, I_S \otimes H_B$). We further assume that $\|H_e\| < \infty$ [10]. Note that this is a physically reasonable assumption, even in situations involving theoretically infinite-dimensional environments (such as the modes of an electromagnetic field), since in practice there is always an upper energy cutoff [11]. We consider “rectangular” pulses [piece-wise constant $H_P(t)$] for simplicity; pulse shaping can further improve our results [1]. An *ideal* pulse is the unitary system-only operator $P(\delta) = \mathcal{T} \exp[-i \int_0^\delta H_P(t) dt]$, where \mathcal{T} denotes time-ordering and $\hbar = 1$ units are used throughout. A *non-ideal* pulse, $U_P(\delta) = \mathcal{T} \exp[-i \int_0^\delta \{H_P(t) + W_P(t) + H_e(t)\} dt]$, includes two sources of errors: (i) Deviations W_P from the intended H_P . Such deviations can be random and/or systematic, generally operator-valued; (ii) The presence of H_e during the pulse.

Periodic DD.— In standard DD one periodically applies a pulse sequence comprised of *ideal, zero-width*

π -pulses representing a “symmetrizing group” $\mathcal{G} = \{P_i\}_{i=0}^{|\mathcal{G}|-1}$ ($P_0 = I$), and their inverses. Let $\mathbf{f}_{\tau_0} = \mathcal{T} \exp[-i \int_0^{\tau_0} H_e(t) dt]$ denote the inter-pulse interval, i.e., free evolution period, of duration τ_0 . The effective Hamiltonian $H_e^{(1)}$ for the “symmetrized evolution” $\prod_{i=0}^{|\mathcal{G}|-1} P_i^\dagger \mathbf{f}_{\tau_0} P_i =: e^{i|\mathcal{G}|\tau_0 H_e^{(1)}}$ is given for a single cycle by the *first-order Magnus expansion*: $H_e^{(1)} \approx H_{\text{eff}} = \frac{1}{|\mathcal{G}|} \sum_{i=0}^{|\mathcal{G}|-1} P_i^\dagger H P_i$ [2]. This result is the basis of an elegant group-theoretic approach to DD, which aims to eliminate a given H_{SB} by appropriately choosing \mathcal{G} [2, 3]. The “universal decoupling” pulse sequence, constructed from $\mathcal{G}_{\text{UD}} := \{\sigma_0, \sigma_1, \sigma_2, \sigma_3\}$, proposed in [2], plays a central role: it eliminates arbitrary single-qubit errors. For this sequence we have, after using Pauli-group identities ($XY = Z$ and cyclic permutations), $\mathbf{p}_1 := e^{i\tau_1 H_e^{(1)}} = \prod_{i=0}^3 P_i^\dagger \mathbf{f}_{\tau_0} P_i = \mathbf{f}_{\tau_0} X \mathbf{f}_{\tau_0} Z \mathbf{f}_{\tau_0} X \mathbf{f}_{\tau_0} Z$, where $\tau_1 = 4\tau_0$. The idea of dynamical symmetrization has been thoroughly analyzed and applied (see, e.g., [7, 12] and references therein). However, higher-order Magnus terms can in fact not be ignored, as they produce cumulative decoupling errors. Moreover, standard PDD is unsuited for dealing with non-ideal pulses [8].

Concatenated DD.— Intuitively, one expects that a pulse sequence which corrects errors at different levels of resolution can prevent the buildup of errors that plagues PDD; this intuition is based on the analogy with *spatially*-concatenated QECC (e.g., [5]). With this in mind we introduce CDD, which due to its *temporal* recursive structure is designed to overcome the problems associated with PDD.

Definition 1 A concatenated universal decoupling pulse sequence: $\mathbf{p}_{n+1} := \mathbf{p}_n X \mathbf{p}_n Z \mathbf{p}_n X \mathbf{p}_n Z$, where $\mathbf{p}_0 \equiv \mathbf{f}_{\tau_0}$ and $n \geq 0$.

Several comments are in order: (i) \mathbf{p}_1 is the “universal decoupling” mentioned above, but one may of course also concatenate other pulse sequences; (ii) One can interpret \mathbf{p}_1 itself as a one-step concatenation: $\mathbf{p}_1 := \mathbf{p}_X Y \mathbf{p}_X Y$, where $\mathbf{p}_X := \mathbf{f} X \mathbf{f} X$ ($\mathbf{f} := \mathbf{f}_{\tau_0}$) and Pauli-group identities have been used. (iii) Any pair, in any order, of unequal Pauli π -pulses can be used instead of X and Z , and furthermore a cyclic permutation in the definition of \mathbf{p}_1 is permissible; (iv) The duration of each sequence is given by $T \lesssim \tau_n := 4^n \tau_0$ (after applying Pauli-group identities); (v) The existence of a minimum pulse interval τ_0 and finite total experiment time T are practical constraints. This sets a physical upper limit on the number of possible concatenation levels n_{max} in a given experiment duration; (iv) Pulse sequences with a recursive structure have also appeared in the NMR literature (e.g., [13]), though not for the purpose of reducing decoherence on *arbitrary* input states. We next present numerical simulations which compare CDD with PDD.

Numerical Results for Spin-Bath Models.— For comparing the performance of CDD vs PDD, we have cho-

sen an important example of solid-state decoherence: a spin-bath environment [14]. This applies, e.g., to spectral diffusion of an electron-spin qubit due to exchange coupling with nuclear-spin impurities [15], e.g., in semiconductor quantum dots [16], or donor atom nuclear spins in Si [17]. Specifically, we have performed numerically exact simulations for a model of a single qubit coupled to a linear spin-chain via a Heisenberg Hamiltonian: $H_e = \omega_S \sigma_1^z + \omega_B (\sum_{a=2}^K \sigma_a^z) + \sum_{a>b \geq 1} j_{ab} \vec{\sigma}_a \cdot \vec{\sigma}_b$. The system spin-qubit is labelled 1; the second sum represents the Heisenberg coupling of all spins to one another, with $j_{ab} = j \exp(-\lambda d_{ab})$, where λ is a constant and d_{ab} is the distance between spins. Such exponentially decaying exchange interactions are typical of spin-coupled quantum dots [16]. The initial state is a random product state for the system qubit and the environment. The goal of DD in our setting is to minimize (the log of) the “lack of purity” of the system qubit, $l \equiv \log_{10}(1 - \text{Tr}[\rho_S^2])$, where ρ_S is the system density matrix obtained by tracing over the environment basis. At given CDD concatenation level n we also implement PDD by using the same minimum pulse interval τ_0 as in CDD and the same total number of pulses $N \lesssim 4^n$; this ensures a fair comparison. In all our simulations we have set the total pulse sequence duration $T = 1$, in units such that $(\omega_S T, \omega_B T, \lambda d_{j,j+1}) = (2, 1, 0.7)$. Longer pulse sequences correspond to shorter pulse intervals τ_0 . Note that we have chosen our system and bath spins to be similar species. Qualitatively, the number of bath spins K had no effect in the tested range $2 \leq K \leq 7$, while quantitatively, and as expected, decoherence rises with K . DD pulses were implemented by switching $H_P = \hbar \sigma_1^\alpha$, $\alpha \in \{x, z\}$, on and off for a finite duration $\delta > 0$; note that $n \leq n_{\text{max}}(T, \delta)$. We define the *pulse jitter* W_P as an additive noise contribution to H_P . It is represented as $W_P^\alpha = \vec{r}^\alpha \cdot \vec{\sigma}_1$, with \vec{r}^α being a vector of random (uniformly distributed) coefficients. We distinguish between *systematic* (W_P^α fixed throughout the pulse sequence, but different for each α) and *random* (W_P^α changing from pulse to pulse) errors.

Our simulation results, shown in Figs. 1-3, compare CDD and PDD as a function of coupling strength, relative jitter magnitude, and number of pulses. Fig. 1, left, compares CDD and PDD at fixed number of pulses. CDD outperforms PDD in the random jitter case with noise levels of up to almost 10%. Fig. 1, right, shows the performance of CDD as a function of jitter magnitude and concatenation level: the improvement is systematic as a function of the number of pulses used. Figure 2 contrasts CDD and PDD in the jitter-free case, as a function of system-bath coupling j . As predicted in the analytical treatment below, CDD offers improvement compared to PDD in decoherence reduction over a wide range of j values. Figure 3 compares CDD and PDD as a function of systematic jitter. Superior performance of CDD is particularly apparent. These results establish the advantage

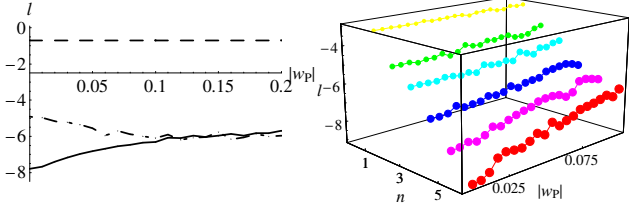


FIG. 1: Left: Performance of CDD (solid line, $n = 4$) vs PDD (dot-dashed line) as a function of *random* jitter fraction $|w_P| := \|W_P\| / \|H_P\|$, with pulse-width $\delta = 10^{-5}T$, coupling strength $j = .2/T$ (T is the total evolution time), and number of bath spins $K = 2$, averaged over 90 jitter realizations. For comparison, the horizontal dashed line corresponds to free evolution. Right: CDD as a function of random jitter fraction $|w_P|$ and concatenation level n . The vertical axis denotes $l = \log_{10}(1 - \text{purity})$ here and in Figs. 2 and 3.

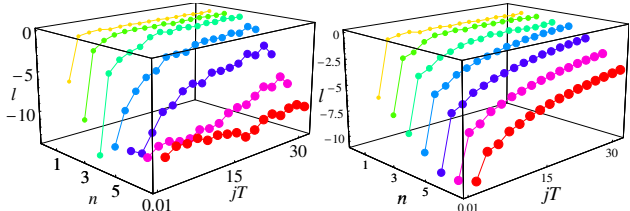


FIG. 2: CDD (left) and PDD (right), as a function of system-bath coupling j ; pulse width $\delta = 10^{-4}T$, number of bath spins $K = 5$, and without jitter ($W_P = 0$). Note the l -axis scale difference between CDD and PDD.

of CDD over PDD in a model of significant practical interest, subject to a wide range of experimentally relevant errors. We now proceed to an analytical treatment.

Imperfect decoupling.— Consider DD pulse sequences composed of ideal pulses. Let us partition H_e as $H_e = H_X^\perp + H_X^\parallel$, where $H_X^\perp = Y \otimes B_y + Z \otimes B_z$ and $H_X^\parallel = X \otimes B_x + H_B$. The super/subscripts \perp, X and \parallel, X correspond to terms that anti-commute and commute with $X \otimes I_B$, respectively. Thus the effect of $p_X = fXfX$ in PDD can be viewed as a *projection* of H_{SB} onto the component “parallel” to X , i.e., H_X^\parallel . For the Y pulses in

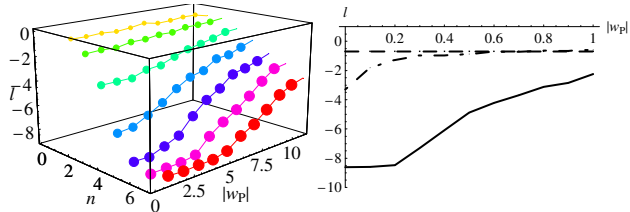


FIG. 3: Left: CDD performance as a function of concatenation level and *systematic* jitter. The pulse width $\delta = 10^{-4}T$, number of bath spins $K = 5$, $jT = 15.0$, averaged over 7 – 80 realizations (more realizations for higher n). Right: CDD (solid line) vs PDD (dot-dashed line) as a function of systematic jitter for $n = 5$, $\delta = 10^{-5}T$, $K = 5$, $j\tau_0 = 3.0$, averaged over 14 – 80 realizations. The dashed line is pulse-free evolution. CDD performance is unaffected up to $\sim 20\%$ jitter level.

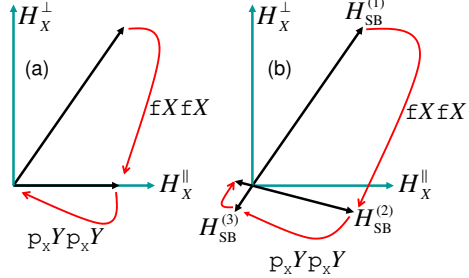


FIG. 4: Projections involved in DD. (a) Perfect cancellation in first-order Magnus case. (b) Extra rotation induced by higher-order Magnus terms, and effect of concatenation.

$p_X = p_X Y p_X Y$ we can similarly write $H_X^\parallel = H_Y^\perp + H_Y^\parallel$, where \perp, Y (\parallel, Y) denotes anti-commutation (commutation) with Y , whence $H_Y^\parallel = H_B$. Then the role of the Y pulses is to project H_X^\parallel onto H_Y^\parallel , which eliminates H_{SB} altogether, i.e., transforms $H_e = H_{SB} + H_B$ into a “pure-bath” operator H_B . This geometrical picture of two successive projections is illustrated in Fig. 4(a). However, these projections are imperfect in practice due to second-order Magnus errors. Indeed, instead of a sequence such as $fXfX$, one has, after pulse $P_{i=X,Y}$, $I_{E,i} := \exp[-i\tau(H_i^\parallel - H_i^\perp)] \exp[-i\tau(H_i^\parallel + H_i^\perp)]$, where $H_e = H_i^\parallel + H_i^\perp$, and we have accounted for the sign-flipping due to P_i . Using the BCH formula (e.g., [18]), we approximate the total unitary evolution as $I_{E,i} = \exp[-i(2\tau)H_{\text{eff},i} + O(\lambda_i^3)]$, where $H_{\text{eff},i} := \mathcal{D}_{P_i}(\tau)[H_e] = e^{-i\tau H_i^\perp/2} H_i^\parallel e^{i\tau H_i^\perp/2}$, where $\lambda_i^3 := \tau^3 \|H_i^\perp\|^2 \|H_i^\parallel\|$, and it is assumed that, since $\|H_e\| < \infty$, one can pick τ such that $\lambda_i \ll 1$. The mapping $\mathcal{D}_{P_i}(\tau)[H_e]$ clearly has a geometric interpretation as a projection that eliminates H_i^\perp , followed by a rotation generated by H_i^\perp . *This rotation produces extra system-bath terms besides H_i^\parallel , hence imperfect DD.* This is illustrated in Fig. 4(b): in the first-order Magnus approximation the transition from $H_{SB}^{(2)}$ to $H_{SB}^{(3)}$ suffices to eliminate H_{SB} , i.e., $H_{SB}^{(3)} = 0$. But in the presence of second-order Magnus errors $H_{SB}^{(3)} \neq 0$. The difference between CDD and PDD is precisely in the manner in which this error is handled: in PDD the $H_{SB}^{(3)}$ error accumulates over time since the same procedure is simply repeated periodically. However, in CDD the process of projection+rotation is continued at every level of concatenation, as suggested in Fig. 4(b) (red arrow above $H_{SB}^{(3)}$). In CDD, $H_{SB}^{(m)}$ is shrunk with increasing m , in a manner we next quantify.

Convergence of CDD in the limit of zero-width pulses.— Decoupling induces a mapping on the components of H_e . For a single qubit, writing $H_e = \sum_{\alpha=x,y,z} \sigma_\alpha \otimes B_\alpha$, we have $H_e \xrightarrow{p_1} H_e^{(1)} = \sum_\alpha \sigma_\alpha \otimes B_\alpha^{(1)}$, where a second-order Magnus expansion yields:

$B_0^{(1)} = B_0$, $B_x^{(1)} = i\tau_0[B_0, B_x]$, $B_y^{(1)} = i\tau_0\frac{1}{2}([B_0, B_y] - i[B_x, B_z])$, $B_z^{(1)} = 0$. Let us define $\beta := \|B_0\|$ and $J := \max(\|B_X\|, \|B_Y\|, \|B_Z\|)$, where we assume $J < \beta < \infty$ [19]. Comparing with the model we have used numerically, $J = O(\lambda)$ and $\beta = O(\omega_B)$. It is possible to show that a concatenated pulse sequence p_n can still be consistently described by a second-order Magnus expansion at all levels of concatenation, provided the (sufficient) condition $\tau_n\beta \ll 1$ is satisfied [20]. We can then derive the recursive mapping relations for $H_e^{(n-1)} \xrightarrow{p_n} H_e^{(n)} = \sum_{\alpha} \sigma_{\alpha} \otimes B_{\alpha}^{(n)}$: $B_0^{(n \geq 0)} = B_0$, $B_x^{(n \geq 1)} = (i\tau_{n-1})[B_0, B_x^{(n-1)}]$, $B_y^{(n \geq 2)} = \frac{1}{2}(i\tau_{n-1})[B_0, B_y^{(n-1)}]$, $B_z^{(n \geq 1)} = 0$. The propagator corresponding to the whole sequence is $\exp(-i\tau_n H_e^{(n)})$, which in the limit of ideal performance reduces to the identity operator. These results for $B_{\alpha}^{(n)}$ allow us to study the convergence of CDD, and bound the success of the DD procedure, as measured in terms of the fidelity (state overlap between the ideal and the decoupled evolution). This fidelity is given by [6]

$$f_n \approx 1 - \|\tau_n \tilde{H}_e^{(n)}\|^2 \approx 1 - (\tau_n h^{(n)})^2 =: 1 - (\Phi_{\text{CDD}})^2, \quad (1)$$

where \tilde{H} is the system-traceless part of H , and $h^{(n)} := \max\{\|B_x^{(n)}\|, \|B_y^{(n)}\|\}$. We find that

$$\Phi_{\text{CDD}} \leq (\beta T / N^{1/2})^n (JT), \quad (2)$$

where $T = N\tau_0 \lesssim \tau_n = 4^n\tau_0$ is the total sequence duration, comprised of N pulse intervals. In contrast, $\Phi_{\text{PDD}} = Th^{(1)}$ yields

$$\Phi_{\text{PDD}} = 2(\beta\tau_0)(JT) = 2(\beta T / N)(JT). \quad (3)$$

Note that for $N = 4$, $\Phi_{\text{CDD}} = \Phi_{\text{PDD}}$ as expected. There is a physical upper limit to the number of concatenation levels, imposed by the condition $\beta\tau_n \ll 1$. Using this condition in the form $\beta = c/T$, where c is some small constant (such as 0.1), and fixing the value of β , we can back out an upper concatenation level $n_{\text{max}} = -\log_4 \frac{\beta\tau_0}{c}$; inserting this into Eq. (2) we have $\Phi_{\text{CDD}} \leq (c\beta\tau_0)^{-\frac{1}{2}\log_4 \frac{\beta\tau_0}{c}} (JT)$. We can now compare the CDD and PDD bounds in term of the final fidelity:

$$\frac{1 - f_{\text{CDD}}}{1 - f_{\text{PDD}}} \leq \frac{(c\beta\tau_0)^{-\log_4 \frac{\beta\tau_0}{c}}}{4(\beta\tau_0)^2} \xrightarrow{\beta\tau_0 \rightarrow 0} 0. \quad (4)$$

This key result shows that CDD converges super-polynomially faster to zero in terms of the (physically relevant) parameter $\beta\tau_0$, at fixed pulse sequence duration. However, it is important to emphasize that our bound on Φ_{CDD} is unlikely to be very tight, since we have been very conservative in our estimates (e.g., in applying norm inequalities and estimating convergence domains). Indeed, in our simulations (above) $\beta\tau_n \approx 2$, which is beyond our conservatively obtained convergence domain.

Finite width pulses.— We now briefly consider the more realistic scenario of rectangular pulses $\mathcal{T} \exp[-i \int_0^{\delta} \{H_P(t) + H_e(t)\} dt]$ of width $\delta \ll \tau_0$. In this case we can derive a modified form of the condition $\beta\tau_n \ll 1$, required for consistency (of using a second-order Magnus expansion at all levels of concatenation) [20]:

$$c\tau_n\beta + d\frac{\delta}{\tau_n} \ll 1, \quad (5)$$

where $c, d \sim 1$ are pulse sequence-specific numerical factors. The consistency requirement (5) validates the analysis of convergence of CDD for $\delta \neq 0$, and we can reproduce the advantage of CDD over PDD for $\delta = 0$ [manifest in Eq. (4)]. As expected Eq. (5) imposes a more demanding condition on the total duration τ_n , at fixed bath strength β . While Eq. (5) cannot be called a threshold condition (in analogy to the threshold in QEC), since it depends on the total sequence duration, it does provide a useful sufficient condition for convergence of a finite pulse-width CDD sequence, and introduces the concept of error per gate which is fundamental in QEC.

Conclusions and outlook.— We have shown that concatenated DD pulses offer superior performance to standard, periodic DD, over a range of experimentally relevant parameters, such as system-bath coupling strength, and random as well as systematic control errors. Here we have addressed the *preservation* of arbitrary quantum states. Quantum *computation* can in principle be performed, using CDD, over encoded qubits by choosing the DD pulses as the generators of a stabilizer QECC, and the quantum logic operations as the corresponding normalizer [21, 22]. Another intriguing possibility is to combine CDD and high-order composite pulse methods [23].

Financial support from the DARPA-QuIST program (managed by AFOSR under agreement No. F49620-01-1-0468) and the Sloan Foundation (to D.A.L.) is gratefully acknowledged.

- [1] R. Freeman, *Spin Choreography: Basic Steps in High Resolution NMR* (Oxford University Press, Oxford, 1998).
- [2] L. Viola, E. Knill and S. Lloyd, Phys. Rev. Lett. **82**, 2417 (1999).
- [3] P. Zanardi, Phys. Lett. A **258**, 77 (1999).
- [4] E. Knill, R. Laflamme, and L. Viola, Phys. Rev. Lett. **84**, 252 (2000).
- [5] A.M. Steane, Phys. Rev. A **68**, 042322 (2003).
- [6] B.M. Terhal and G. Burkard, Phys. Rev. A **71**, 012336 (2005).
- [7] P. Facchi *et al.*, Phys. Rev. A **71**, 022302 (2005).
- [8] L. Viola and E. Knill, Phys. Rev. Lett. **90**, 037901 (2003).
- [9] H. Rabitz *et al.*, Science **288**, 284 (2000).

- [10] We use the *spectral radius* $\|A\| := \max_{\langle\psi|\psi\rangle=1} |\langle\psi|A\psi\rangle|$; a convenient unitarily-invariant operator norm, which, for normal operators, coincides with the largest absolute eigenvalue.
- [11] This has been observed also in QECC work dealing with general error models [4, 6], but as has been pointed out there, if $\|H_e\| = \infty$ it must be appropriately redefined.
- [12] L. Viola, J. Mod. Optics **51**, 2357 (2004).
- [13] U. Haeberlen and J. S. Waugh, Phys. Rev. **175**, 453 (1968); H.M. Cho, R. Tycko, and A. Pines, Phys. Rev. Lett. **56**, 1905 (1986).
- [14] N.V. Prokof'ev and P.C.E. Stamp, Rep. Prog. Phys. **63**, 669 (2000).
- [15] R. de Sousa, S. Das Sarma, Phys. Rev. B **68**, 115322 (2003).
- [16] G. Burkard, D. Loss and D.P. DiVincenzo, Phys. Rev. B **59**, 2070 (1999).
- [17] B.E. Kane, Nature **393**, 133 (1998).
- [18] S. Klarsfeld, J.A. Oteo, J. Phys. A **22**, 4565 (1989).
- [19] This assumption is made to simplify some of our convergence arguments; while it is not essential, it is reasonable, since we expect only a small number of bath degrees of freedom to be coupled to a given qubit, whereas no restriction exists on the bath self-Hamiltonian
- [20] K. Khodjasteh and D.A. Lidar, in preparation.
- [21] M.S. Byrd and D.A. Lidar, Phys. Rev. Lett. **89**, 047901 (2002).
- [22] M.S. Byrd and D.A. Lidar, J. Mod. Optics **50**, 1285 (2003).
- [23] K.R. Brown, A.W. Harrow, I.L. Chuang, Phys. Rev. A **70**, 052318 (2004).